Journal of Science and Sustainable Development (JSSD), 2023, 11(2), 94-110

ISSN: 2304-2702 (print); 2414-4479 (online)
DOI: https://doi.org/10.20372/au.jssd.11.2.2023.0467

RESEARCH PAPER

Biosynthesization of ZnO/CuO Nanocomposites in Orange Peel Crude Extract for Antibacterial Activities

Tibebu Alemu[1*], Girmaye Asefa[1], Musa Shumbura[1], Asefa Kenani[2], Andualem Merga Tullu[3]

[1]*Department of Chemistry, College of Natural and Computational Sciences, Ambo University, Ambo, Ethiopia*
[2]*Department of Biology, College of Natural and Computational Sciences, Ambo University, Ambo, Ethiopia*
[3]*Faculty of Chemistry, Silesian University of Technology, Marcina Strzody 9, 44-100 Gliwice, Poland.*
***Corresponding Author** Email: tibebu.alemu@ambou.edu.et*

Abstract

Nanoparticles (NPs) in particular ZnO and CuO are inorganic nanomaterials used in application areas such as electronics, communication, chemical/biological sensors, cosmetics, environmental remediation, biomedicinal industry, energy preservation, photocatalysis, and microbial growth inhibition. This study focused on the biosynthesis of ZnO NPs, CuO NPs, and ZnO/CuO nanocomposites (NCs) in orange fruit extract to investigate the growth inhibition of gram-positive and gram-negative bacteria. The crystal structure, functional group, and energy band gap of as-synthesized NPs and NCs were characterized with the aid of X-ray diffraction (XRD), Fourier Transform Infrared (FTIR), and Ultra Violet-Visible (UV-Vis) spectroscopic techniques, respectively. Consequently, the XRD results confirmed the formation of a hexagonal wurtzite phase, and the average crystallite sizes of the nanomaterials of 22.71-33.89, 16.46-33.04 and 16.76-26.89 nm for ZnO NPs, CuO NPs, and ZnO/CuO NCs synthesized with and without orange peel extract, respectively while the vibrational stretching obtained around 476 and 564 cm^{-1} confirmed the presence of Zn-O, and Cu-O bond, respectively. The characteristic absorption spectrum observed at 285 nm supported the synthesization of ZnO/CuO NCs within a very narrow energy bandgap. Furthermore, the antibacterial activity of the ZnO/CuO with orange peel extract (WE) NCs, ZnO (WE) and CuO (WE) were significantly higher as compared to that without orange fruit extracts (WoE) NPs/NCs. The results show that the NPs and NCs synthesized WE had a high potential growth inhibition zone against gram-positive bacteria (S. aureus) ranges from 16.67 to 12.00 mm and gram-negative bacteria (P. aeroginosa) ranges 16.00 to 12.30 mm. In this study, we have discovered that the green synthesized ZnO/CuO NCs can be introduced as a promising anti-bacterial agent and so applicable to cure microbial strain-based infectious diseases.

Keywords: Green synthesis routes, bacterial growth inhibition, ZnO/CuO Nanocomposites, inhibition zones, orange peel extract

Introduction

In recent nanobiotechnologies, scientists are able to synthesize nanoparticles (NPs) based materials (Shafique et al., 2020; Shah et al., 2021) since it received great consideration in nanotechnology as a result of their functional response which is fundamentally affected by the crystalline size and surface-to-volume ratio (Lewis and Klibanov, 2005). Predominantly, inorganic nanomaterials (NMs) are the most advantageous functional materials (Mahmood et al., 2023) because of their chemical stability, safety, and biological compatibility (Li et al., 2017; Xiang et al., 2017). For example, prior reports (Cui, Li, Li, and Mao, 2022; Hajiali et al, 2021) signify that the incorporation of functional NMs is paramount important in biomedicals, particularly in speeding up bone transplantation and wound curing. Moreover, the inorganic NMs are very effective in environmental remediation, energy production and the inhibition of bacterial growth (Gold et al., 2018). Nowadays, scholars are developing

chemical and biological resistance techniques against infectious diseases caused by microbial organisms (Bala et al., 2015; Dadi et al., 2019) since using ordinary antimicrobial agents enhances the expansion of numerous drug resistance and generates hostile side effects. These challenges initiated the development of substitutive antibacterial inhibition approaches to cure bacterial diseases (Baker-A et al., 2006) without being toxic to the other tissue. A typical natural products, for instance, aminoglycosides and synthetic antibiotics are frequently used, however, chemically modified compounds are currently used as antibacterial agents (Von et al., 2006). It is mentioned that nanomaterials have been developed for microbial inhibition (Hussain et al., 2023) in particular as antibiotics which have proven their effectiveness in tackling infectious diseases (Huh and Kwon, 2011). In the biomedical area, NPs are preferable (Alsafari et al., 2023) due to their high surface area-volume ratio, initiating new mechanical, chemical, electrical, optical, magnetic and electro-optical which differ from their bulk properties (Whitesides, 2005).

The destruction of bacteria by NPs can be determined by its properties which directly depend on its respective bacterial strains. For instance, E. coli is more sensitive to CuO NPs however, S. aureus and bacillus behave controversially (Baek and An, 2011) while S. aureus and B. subtilis are sensitive to NiO, and ZnO NPs (Lu and Botstein, 2009). On the other hand, fast-growing bacteria are highly vulnerable as compared to slow-growing bacteria to antibiotics as well as to NPs (Hajipour et al., 2012). In order to employ nanoscale devices in particular fields of applications, numerous synthesis approaches have been developed (Abid et al., 2022). For example, green synthesis is among the pertinent techniques because of its environmentally friendly (Albrecht and Raston, 2006) method and could fulfill the huge gaps observed in conventional approaches in avoiding the long-term dispensation, expensive, tedious procedures, and generation of poisonous compounds. Consequently, researchers have intended to develop an appropriate, eco-friendly and efficient synthesis known as the green method for the preparation of NPs (Herlekar and Kumar, 2014). Therefore, the synthesis of metal oxide-based NPs via green routes particularly the incorporation of plant extracts is a simple, economical, and toxic-free method (Bala et al., 2015). The plant extracts are preferred because of their advantages in reducing ability, surface stabilization and capping capability during the synthesis of NPs (Kumar et al., 2020; Thi et al., 2020). For instance, ZnO-NPs is one of an interesting NMs with multifaceted benefits and have been used in revolutionized applications (i.e., electronics, communication, chemical/biological sensors, cosmetics, environmental remediation, biomedicinal industry, energy preservation, textiles, human health, photocatalysis) (Sankapal et al., 2016), gene/drug delivery, nanomedicine (Yoon and Kim, 2006), as bacterial/fungal/diabetic inhibition agent, acaricidal, pediculicidal and larvicidal (Alkaladi and Afifi, 2014). ZnO NP (Rajiv and Venckatesh, 2013) was synthesized in the orange peel extract which possesses a variety of natural anti-oxidants. Rajiv and Venckatesh, (2013) examined the influence of working parameters on its antibacterial activities against S. aureus and E. coli bacterial strains. The report revealed that ZnO NPs are effective towards sterilizing E. coli with inhibition rates >99.9% (Thi et al., 2020). Similarly, MgO and CaO NPs were also prepared to identify their efficacy against E. coli and S. aureus growth inhibition (Sawai, 2003). Alternatively, a p-type semiconductor copper oxide (CuO) having a narrow energy bandgap has been widely utilized for numerous goals as a result of its eco-friendly types, exceptionally stable, and anti-inflammatory/bacterial agent (Hussain et al., 2016), applicability in gas sensor, water reducing agents, super-hydrophobic nature and photocatalytic degradation phenomena (Dey, 2018).

Moreover, the hierarchical metal oxide (MO) NPs such as CuO–ZnO NCs were recently developed as photocatalysts for the degradation of organic dye which was also been employed in several application areas (Liang et al., 2018) due to their high adsorption capability, extra sites for functional moieties and adequate porosity. For example, ZnO–CuO NCs have been green synthesized using Calotropis

gigantean while the synthesized NCs showed superior photocatalytic activity against MB dye and depressed the growth of E. coli and S. aureus stains. A study signifies that such a combination of NPs has verified the potential antimicrobial activity of NCs (Akhavan and Ghaderi, 2010) while it is very dependent on the size and concentration of precursors (Azam et al., 2012). In this regard, the average size of NPs is smaller than bacterial pores which enhances the penetration of bacterial cells (Ahamed et al., 2014).

Despite many efforts that have been shown about the antibacterial activities using MO modified with plant extracts, still it needs detailed investigation (Kumar et al., 2023) with the help of green synthesis of mixed metal oxides. To the best of our knowledge, there is no research employed yet dealing with the green synthesis of ZnO/CuO NCs using orange peel extracts for bacterial growth inhibition. Thus, this research work intended the green synthesis of ZnO NPs and CuO NPs combined nanocomposites (ZnO-CuO NCs) in orange peel extract and study of antibacterial activities against Gram-negative (Pseudomonas aeroginosa) and Gram-positive (Staphylococcus aureus) strains. Here, the orange peel extracts is preferred to synthesize NPs/NCs since it conatains the secondary metabolites with potential reducing ability, surface stabilization and capping power for this particular nanomaterial. The NCs has purposively prepared from the combination of ZnO and CuO NPs in a sense that ZnO NPs is very popular in photocatalysis, drug delivery, nanomedicine and microbial inhibition activities; CuO NPs is widely utilized due to its eco-friendly nature, more stable, antibacterial activities and photocatalytic abilities. Thus, its anticipated that the combination of these NPs in the presence of orange peel extract which possesses a variety of anti-oxidant components such as flavonoids, tannins, reducing sugars, cardiac glycosides, alkaloids, coumarins, O-heterosides, and C-heterosides (Brezo-Borjan, 2023) would result in NCs with the narrow energy bandgap and high surface-to-volume ration so as to enhance the bacterial growth inhibition rates. The prepared NPs and NCs were characterized with UV-Vis, XRD, and FTIR spectroscopy, and the bacterial inhibition mechanism has been also deduced. The current result demonstrated that the as-synthesized NPs and NCs have the potential for growth inhibition for both bacterial strains.

Materials and methods

Chemicals and instruments

Zinc (II) acetate dihydrate, $Zn(CH_3COO)_2.2H_2O$, and copper sulfate pentahydrate, $CuSO_4.5H_2O$ were employed to synthesize ZnO NPs, CuO NPs and ZnO/CuO NCs and sodium hydroxide, NaOH are chemicals used for this study while ethanol was employed as the precipitating agents and washing purposes. Orange peel was taken to synthesize CuO and ZnO NPs using the sol-gel technique. Nutrient broth (NB) was provided by Ambo University, Biology Laboratory while the Agar disc diffusion method was adopted to evaluate the antibacterial activity of NCs. Instruments including UV-Vis Spectroscopy (Cary 60 UV-Vis, Agilent technologies), Fourier Transform Infrared (FTIR, Perkin-Elmer LS-65-Luminescence spectrophotometer), and X-ray Diffraction (XRD, Min flux 600 powder diffractometer Rigaco, USA) were used to characterize the surface properties of nanomaterials.

Collection of orange peel and Preparation of the extract

The orange peel was purposively selected by considering its chelating ability, reducing and capping agent in the process of ZnO NPs, CuO NPs, and ZnO/CuO NCs synthesis. Accordingly, 4 kg of fresh orange fruit was purchased from market in Ambo Town, Oromia Regional State. The orange fruit is washed with tap water to remove the contaminants and rinsed with distilled water (DI) before being peeled and dried. The peel was then placed in an oven for 24 hrs to get dried components. The dried peel was pulverized with a grinder to produce a powder which was further used for the extraction process (Brezo-B., 2023). Then, 30 g of powdered orange peels was dissolved in 300 mL DI followed by stirring for 1 hr at 50 ^oC. Then after, the heated samples was purified

with the help of What man no.1, and the solution hereafter utilized as a plant extract and stored at 4 ^{o}C which was further used for analysis (Kumar et al., 2020).

Preparation of ZnO and CuO NPs

ZnO and CuO NPs were prepared via sol-gel method without orange peel extract (WoE) (Dadi et al., 2019). ZnO (WoE) NPs and CuO NPs (WoE) samples were synthesized by dissolving 2 g of $Zn(CH_3COO)_2.2H_2O$, and 1.6 g of $CuSO_4.5H_2O$ in each 60 mL of DI under constant stirring. After 30 min, 1 M NaOH aqueous solution were added dropwise to each solution for the pH adjustment to 12. The solutions was agitated for an additional 3 hrs. The resultant precipitate is washed by DI and ethanol persistently which then dried at 60 ºC for 24 hrs. The powder was calcinated at 500 $^{\circ}$C for 2 hrs. To the above primary solution, 30 mL of orange peel extracts was added through continuous stirring. Similarly, 1 M NaOH was added into the above solution after 30 min in order to fix the pH to 12. The solution was then held undisturbed for 18 hrs to form a gel followed by washing using DI and ethanol repeatedly. Finally, CuO NP with extracts (WE) and ZnO NPs (WE) were obtained once the gel has dried in a vacuum oven at 60 °C and calcinated at 500 ºC for 2 hrs (Mohammadi-Aloucheh, 2018).

Reaction mechanism in the synthesization of ZnO and CuO NPs

Scheme 1 displays the possible reaction mechanism during the synthesis process of ZnO and CuO NPs using orange peel extract. The bioactive components that exist in orange peel extract could act as ligand agents. Then, the complex compounds would be formed between the OH group of the organic molecules and Zn^{2+} ions. The corresponding nanoparticles formed and stabilized through nucleation process while the mixture of organic parts would be decomposed upon calcination resulting in the formation of ZnO NPs, Scheme 1(a) (Thi et al., 2020). Similarly, CuO NPs was synthesized as the phytochemicals components in extracts play the reducing process to convert Cu^{2+} ions to Cu NPs. Finally, Cu^{0} gets oxidized to CuO NPs upon calcination, Scheme 1(b) (Ahmed et al., 2022) and also the organic components are used as capping agents to prevent the NPs agglomerations (Veisi et al., 2021).

Preparation of ZnO/CuO NCs

ZnO/CuO (WoE) NCs were synthesized using 2 g of $Zn(CH_3COO)_2.2H_2O$ and 1.6 g of $CuSO_4.5H_2O$ separately dissolved in 60 mL of DI. 60 mL $CuSO_4.5H_2O$ solution is added dropwise into 60 mL of $Zn(CH_3COO)_2.2H_2O$ solution. After constant agitation for 30 min, the pH of the solution is fixed to 12. It was then allowed to quiescent for 18 hrs so as to form gel via washing by DI and ethanol. The gel is then dried at 60 °C and calcinated at 500 ºC for 2 hrs in order to prepare ZnO/CuO (WoE) NCs. ZnO/CuO (WE) NCs were synthesized via adding 30 mL of the orange peel extract to the solution containing ZnO/CuO NCs.

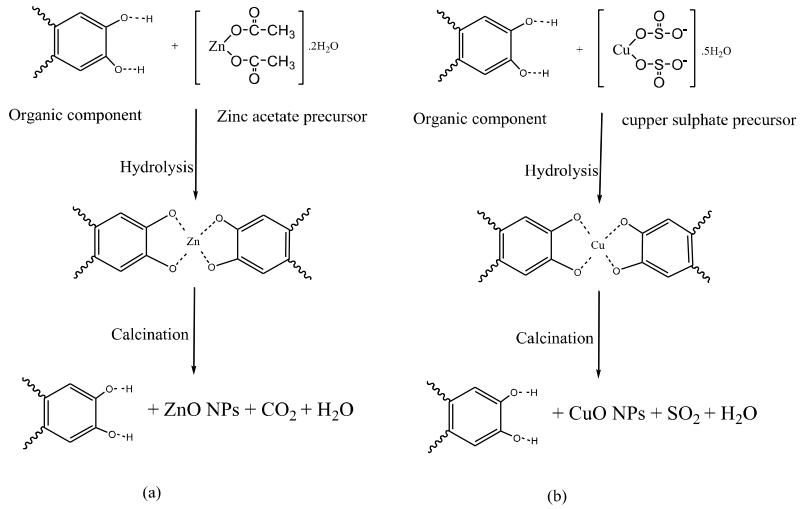

Scheme 1. The reaction mechanism during the formation of (a) ZnO NPs and (b) CuO NPs.

The required NCs is obtained by adjusting the pH of the solution to 12 which was kept for 18 hrs to form a gel. The gel was then constantly washed by DI, dried at 60 °C, and finally calcinated at 500 °C for 2 hrs (Mohammadi-Aloucheh, 2018).

The Characterization of ZnO NPs, CuO NPs, and ZnO/CuO NCs

The colloidal solution of ZnO NPs, CuO NPs, and ZnO/CuO NCs were tested for optical absorption properties with the help of UV-Vis Spectrophotometer over a wavelength of 200-800 nm to determine their energy band gaps. The quartz cuvet was used as a sample holder and distilled water as a blank solution. The functional group of as-synthesized NPs and NCs were studied by FTIR spectrometer (Perkin-Elmer LS-65- Luminescence spectrometer) in 4000–400 cm^{-1} wavenumber. The crystalline structure and grain average size of nanoparticles/composites was revealed by powder X-ray diffractometer (XRD, Min flux 600 powder diffractometer Rigaco, USA) with Cu Kὰ radiations (k =0.154060 nm) in 2θ of 10 - 80°. The average crystalline size of as-synthesized NPs/NCs was determined by Debye-Scherrer equation (Eq. 2.1) (Gawade et al., 2017):

$$D = \frac{0.9\lambda}{\beta cos\theta} \qquad (2.1)$$

where 0.9 is Scherrer's constant, λ is the wavelength of radiation equivalent to 0.15406 nm, β is peak width at half maximum, and θ is Bragg's angle.

Evaluation of antibacterial activities of the nanomaterials

Antibacterial activity of as-synthesized nanomaterials were done via taking two human pathogenic bacterial strains (*Staphylococcus aureus AT2228* (gram-positive) which was obtained from Ethiopian Public Health Institute, and *Pseudomonas aeroginosa* (gram-negative) local clinical isolate (isolated in Biology Laboratory, Department of Biology , College of Natural and Compuational Sciences, Ambo University). Agar well diffusion method was adopted for an evaluation of the antibacterial activity of nanomaterials. Muller Hinton (MH) Agar plates were prepared, sterilized, and solidified. After solidification, 10^6 CFU of bacterial cultures was swamped on solidified MH Agar plates. Inoculums were

prepared by mixing a few microbial colonies with 4 mL of sterile peptone water and comparing the turbidity with that of the standard 0.5 McFarland solution which is equivalent to 10^6cfu/ml of bacteria (Balouiri *et al*., 2015). Five wells were cutout in the agar layer of the plate using an aluminum borer of 6 mm diameter for each synthesized NPs (Prabakaranand Gunawardena, 2012). In the case of ZnO (WE, WoE), CuO (WE, WoE), and ZnO/CuO (WE, WoE) synthesized nanomaterials were prepared to determine the effective concentration for bacteriostatic/bactericidal. Then, 50 ml of each of the synthesized nanoparticles, positive control (Cloxacillin), and negative control (DMSO) were dropped into the wells using a micropipette which has been incubated at 37 °C for 18 hrs. At the verge of incubation time, the bacterial inhibition activities of as-synthesized NPs were checked through observing and the zone of inhibition was measured by ruler (mm) and the data was recored.

Results and Discussion

Analysis of Crystal Structure

Fig. 1 represents XRD spectra of ZnO (WE, WoE), CuO (WE, WoE) and ZnO/CuO (WE, WoE) NCs. The XRD patterns of ZnO (WoE) NPs are located at 31.87, 34.53, 36.36, 47.64, 56.69, 62.96, 66.47 and 68.04 diffraction angle which corresponds to miller indeces of (100), (002), (101), (102), (110), (103), (200) and (112) indicated the presence of pure ZnO (WoE) NPs as it was agreed with the result observed and assigned to JCPDS file no. 361451 (**Bala et al., 2015**). The XRD spectra corresponding to ZnO (WE) were observed at 31.82, 34.47, 36.29, 47.58, 56.64, 62.42, 62.91, 66.43 and 68.04 diffraction angle confirmed the existence of extract so that it does not affected the crystallinity of ZnO NPs. In this regard, ZnO (WoE, WE) samples corresponded to hexagonal crystalline phase as reported in the previous studies (**Arakha et al., and 2015**). This result demonstrated that all the characteristic peaks of ZnO (WoE, WE) NPs were similar before and after the addition of orange peel extracts with no impurities existing in synthesized NPs (**Bala et al., 2015**).

The average crystalline size (Eq. 2.1) for ZnO (WoE) and ZnO (WE) were calculated using three intensive peaks (**Batool et al., 2022**). Accordingly, the obtained crystallite size were 33.89 and 22.71 nm, respectively (Table 1). The calculated values of ZnO (WE) NPs was smaller as compared to ZnO (WoE) NPs which signifies that the orange peel extract would assist the reduction of Zn^{2+} ions to Zn NPs with smaller particle size. XRD pattern for CuO (WoE) NPs showed peaks at 2θ = 33.65, 38.86, 48.88, 58.39, 61.65, 66.34, 68.15, and 75.56º corresponding to (110), (200), (202), (020), (113), (311), (220) and (004) planes. As no additional peaks were emerged which related to other phases, all the diffraction patterns are indexed to indicate the typical monoclinic structure of the NPs. In addition, the XRD pattern for as-synthesized CuO (WE) NPs peaks were noticed at 2θ = 32.24, 35.65, 38.86, 48.88, 58.39, 61.65, 66.34, 68.15 and 75.56º corresponding to (110), (111), (200), (202), (020), (113), (311), (220) and (004) planes which agree with JCPDS Card No. 80-1916.

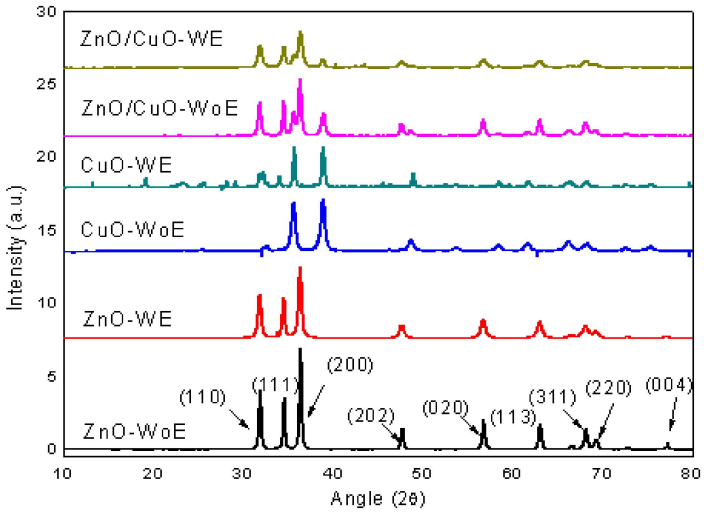

Figure 1. XRD spectrum of ZnO NPs, CuO NPs, and ZnO/CuO NCs with and without orange peel extract.

Similarly, the average crystalline size for CuO (WoE) and CuO (WE) are found to be 33.04 and 16.46 nm, respectively (Table 1) which followed the same trends of ZnO (WoE, WE) (Hasan et al., 2022). The diffraction peaks of ZnO/CuO (WoE) NCs was observed at 31.81, 34.47, 36.29, 38.87, 47.58, 56.64, 62.90, and 68.02º while the diffraction angle was observed at 31.86, 34.51, 36.34, 38.82, 47.64, 56.66, 62.93 and 68.05 º for ZnO/CuO (WE) NCs. From the results, the green synthesized ZnO–CuO (WoE, WE) NCs are well-matched with the standard value of JCPDS card No. 3–888 and 5–661 (Mohammadi-Aloucheh, 2018) confirming the prepared NCs from the combination of NPs are crystal in nature. Furthermore, the absence of extra phases could signify that the as-synthesized NCs is pure in phase. The calculated the average crystalline from (Eq. 2.1) (Naik et al., 2018) for ZnO-CuO NCs is equals to 26.89 and 16.76 nm, respectively. It is evident that, the corresponding crystalline size of ZnO/CuO (WE) NCs was smaller than that ZnO/CuO (WoE) (Table 1). This difference might be raised as various functional groups such as O-H, C-H, O–CH_3, CHO, and COOH existed within the orange peel extract (Multari et al., **2020**). On top of that, the phytochemical constituents presented in the plant extracts could trigger the reduction of Zn^{2+} and Cu^{2+} ions and reduce the crystalline size of as-synthesized NPs (Bala et al., 2015).

Table 1. Summary of crystalline size calculation data obtained from XRD spectra

Photocatalyst	2θ	θ	cosθ	β (FWHM)	FWHM (radian)	D (nm)	Average (nm)	
ZnO-WoE	36.36	18.18	0.95009	0.2635	0.004598943	33.1304	33.89	
	31.87	15.93	0.96157	0.2684	0.004684464	32.137		
	34.53	17.27	0.95494	0.2384	0.004160865	36.4324		
ZnO-WE	36.29	18.15	0.95026	0.4164	0.007267551	20.9613	22.71	
	31.81	15.91	0.96171	0.407	0.00710349	21.1902		
	34.47	17.24	0.95509	0.3341	0.005831145	25.9925		
CuO-WoE	38.86	19.43	0.94305	0.31	0.005410521	28.371	33.04	

	35.65	17.82	0.95201	0.2602	0.004541347	33.4829	
	32.24	16.12	0.96069	0.2317	0.004043928	37.2617	
CuO-WE	38.84	19.42	0.94311	0.5271	0.00919963	16.6845	16.46
	35.57	17.79	0.95221	0.4912	0.008573057	17.733	
	48.64	24.32	0.91125	0.6084	0.010618583	14.9604	
ZnO/CuO-WoE	36.29	18.15	0.95026	0.3565	0.006222099	24.4832	26.89
	34.47	17.24	0.9551	0.2699	0.004710644	32.1752	
	31.81	15.9	0.96172	0.3589	0.006263987	24.0298	
ZnO/CuO-WE	36.34	18.85	0.9464	0.5476	0.009557427	15.1463	16.76
	31.86	15.93	0.27082	0.5004	0.008733631	16.575	
	34.51	17.25	0.955	0.447	0.007801625	18.5551	

Analysis of functional group

Fig. 2 represents the FT-IR spectrum of ZnO (WoE, WE), CuO (WoE, WE) NPs, and ZnO/CuO (WoE, WE) NCs. Accordingly, the weak absorption spectrum determined at 3410 cm^{-1} represented stretching vibrations of O-H bond in the aforementioned samples (Gayenet al., 2008). The current finding agree with the previous reports (Hashmi, 2021) on the existence of fundamental functional group of NPs/NCs. Accordingly, the presence of aromatic compounds in the samples containing plant extracts was demosntrated C=C stretching, C–H stretching, and C=C–C asymmetric stretching bands which corresponding to 1100, 1140 and 1450 cm^{-1}, respectively (Awwad and Abdeen, 2012). In addition, the bending vibration of –C–OH, stretching vibration of –N-H_2 and stetching vibration of –C=O groups in alcohol, secondary amine and conjugated aromatic ring, respectively are observed at 850 cm^{-1} (Mukherjee et al., 2012). Alternatively, the FTIR spectra of ZnO (WoE, WE) and ZnO/CuO (WoE, WE) displayed at 424 cm^{-1} are attributed to the stretching vibration of Zn–O (Das et al., 2012). Prior study revealed that the presence of polysaccharide carbohydrates has the adequate binding power with metals (Zn, Cu) and generate layers on its surface in order to avoid agglomeration in the reaction medium (Sawai, 2003). Similarly, the distinct peak generated at 450 cm^{-1} represent the vibration of Cu–O bond in CuO (WoE, WE) and ZnO/CuO (WoE, WE) NPs and NCs, respectively.

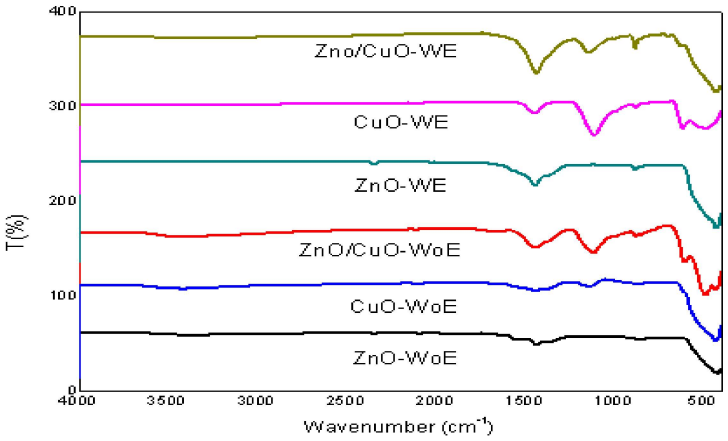

Figure 2. FTIR spectra of as-synthesized nanomaterials with and without extracts

Moreover, the substantial absorption bands corresponding to ZnO/CuO (WoE, WE) NCs existed at 424 cm^{-1} and 450 cm^{-1} are ascribed Zn–O and Cu–O stretching vibrations, respectively (Kiwi and Nadtochenko, 2005). As a consequence, the anticipated functional groups were confirmed from the FTIR spectra indicating that the NPs and NCs were successfully synthesized. In addition, the spectra of samples containing orange peel extract provided more intensive peaks as compared to samples without extract ensured the presence of secondary metabolite impact the stretching vibration of the NPs/NCs.

UV-Vis Absorption Analysis

Fig. 3 demonstrate UV-Vis spectrum of as-synthesized NPs and NCs. The spectrum showed the characteristics absorbance bands of nanomaterials realize the formation of NPs and NCs. The result signified that the synthesized NPs and NCs with orange peel extract are suitable to complete the reduction of Zn^{2+} and Cu^{2+} to ZnO and CuO NPs respectively. The absorption wavelength may be adhered to the energy band gap (E_g) of the synthesized ZnO (WoE, WE) NPs, CuO (WoE, WE) NPs, and ZnO/CuO (WoE, WE) NCs. Nevertheless, the band edges of NCs are more significant, denoting the addition of CuO creates extra states in the band gap of ZnO. The energy band gap of as-synthesized nanomaterials determined using Eq. 2, (Alemu T. et al., 2022):

$$E_g = {}^{hc}/_{\lambda} \quad (2.2)$$

where, h is Planck's constant = 6.63 x 10^{-34} m^2 kg s^{-1}, c is speed of light = 3.00 x 10^8 ms^{-1}, λ is maximum absorption wavelength in UV region. The E_g value for ZnO (WoE, WE) NPs, CuO (WoE, WE) NPs, and ZnO/CuO (WoE, WE) NCs were calculated ranging between 3.02 to 2.70 eV which is slightly lower than un-doped ZnO NPs (3.31 eV) and CuO NPs (3.28 eV) as reported by (Shamsuzzaman et al., 2014, Khan et al., 2013) and even lower than the theoretical values of 3.37eV (Deviet al., 2014). Conversely, the energy gap has significantly declined for the NCs and further improved for NPs treated with extracts i.e., 3.02, 2.84, 2.81 and 2.70 eV for CuO (WoE) NPs, CuO (WE), ZnO/CuO (WoE) and ZnO/CuO (WE) NCs respectively. The result indicates that the UV-Vis absorption spectrum for synthesized samples absorbs at a specific wavelength for each nanomaterial. Owing to the smaller E_g, the electron is simply excited from VB to CB which depends on the particle size, oxygen deficiency, surface coarseness, and lattice strain of NPs (Fahmy and Cormier, 2009). Therefore, UV-Vis spectroscopic characterization has specified the preparation of nano-sized ZnO, CuO and ZnO/CuO with and without orange peel extracts with significant optical absorption ability.

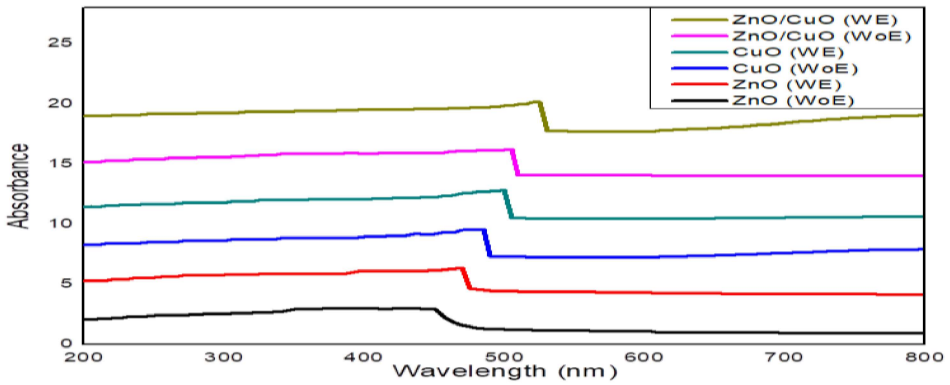

Figure 3. UV-Vis spectra of ZnO (WoE, WE) NPs, CuO (WoE, WE) NPs, and ZnO/CuO (WoE, WE) NCs.

Study of antibacterial activity

An antimicrobial activities of CuO (WoE, WE) NPs, ZnO (WoE, WE) NPs, and ZnO/CuO (WoE, WE) NCs were examined for anti-bacterial activity against two human pathogenic bacterial strain i.e., gram-positive (*S. aureus)* and gram-negative (*P. aeroginosa*) by means of agar well diffusion technique (Fig. 4 and 5). In this study, orange peel extract was used since its phytochemicals become specific in the synthesis of nanoparticles and play a role in reducing and capping purposes (Faisal et al., 2021). As an indicator of how effectively nanomaterials and antibiotics combat bacteria, the ZOI that developed around the wells displayed the clearance of bacteria with control samples (Cloxacillin and DEMSO). The antibacterial effect of nanomaterials against both bacteria compared with control samples showed varied ZOI diameters at the same concentration level of different NPs (Table 2). The ZOI reflect the bacteria's susceptibility to toxic agents so that the disinfectant sensitive strains show larger ZOI radius which is opposite to resistant strains. Among the three NPs/NCs, the antibacterial activities of ZnO/CuO (WE) NCs were measured and showed a good response against *S. aureus* with an average maximum ZOI of 16.67 mm while against *P. aeroginosa* showed relatively lower average ZOI which is 15.33 mm after 18 hrs incubation times. This indicates that ZnO/CuO (WE) NCs are more effective in *S. aureus* than *P. aeroginosa*. ZnO/CuO (WoE) NCs recorded 13.70 and 15.30 mm antibacterial ZOI against *S. aureus* and *P. aeroginosa,* respectively. The findings revealed that the bacterial susceptibility to the aforementioned NPs and NCs were found vary relying on microbial species and presence of orange peel extract.

The well filled with the negative control (DMSO) did not show any ZOI whereas the well filled with the positive control (Cloxacillin) showed the highest ZOI. Practically, the antibacterial activity primarily depends on the reactive oxygen species (ROS), NPs surface area, and sizes. ZnO/CuO NCs generate ROS such as HO*, O_2^{*-}, O_2, and α-O through the Fenton reaction. This radical formation could abolish the bacteria via lipid peroxidation, DNA damage, and protein oxidation (Kumar et al., 2020). A similar study was conducted using the ZnO/CuO NCs to investigate its performance against *S. aureus* and *E. coli*. The ZOI formed by NCs has been showing substantial degree of inhibition for both bacterial strains as compared to standard antibiotic ciprofloxacin (Lingaraju, N., 2019). Similarly, the antibacterial efficacy of ZnO-NPs synthesized using a medicinal plant was investigated and the biosynthesized NPs attain fundamental capping and stabilizing agents originated from plant extracts (Hussain and Hasan, 2023**,** Khan et al., 2016**,** Kumar et al., 2017). In accordance, ZnO (WE) NPs have antibacterial ZOI of 14.7 and 16 mm against *S. aureus* and *P. aeroginosa* while ZnO (WoE) NPs have inhibited bacteria to about 12.7 and 15 mm against *S. aureus* and *P. aeroginosa,* respectively. This indicates that both ZnO (WoE, WE) NPs are more effective for *P. aeroginosa* than *S. aureus* which also works for CuO (WE) NPs. Therefore, the as-syntheisized NPs were observed with effecive inhibition of Streptomyces strain in a dose-dependent way (Faisal et al., 2021). In current study, the bacterial inhibition mechanisms entails the formation of reactive oxygen species (ROS) including hydrogen peroxide (H_2O_2), hydroxyl radicals ($^*OH$), peroxide (O_2^{2-}) (Nair et al., 2009) and reactive ions of NPs (Kasemets et al., 2009**)** are among the driving active species. These reactive species are speed up the demolition of cellular constituents of *S. aureus* and *P. aeroginosa* (Lipovsky et al., 2011). In this regard, the ZnO nanotoxicity is due to the dissolution of ZnO NPs into Zn^{2+} ions (Zhu and Lin, 2011) as well as formation of Cu^{2+} ions. Jiang et al. (Jiang and Xing, 2009) and Sawai (Sawai, 2003) reported the role of Zn^{2+} in ZnO nanotoxicity is negligible due to low concentrations of solubilized Zn ions. Ultimately, the bacterial membrane permeability could be altered through the accumulation and spreading of NPs in the cell membrane (Díaz-V. et al., 2011).

Table 2. Antibacterial activity of nanomaterials with/without orange peels extract applied to two human pathogenic bacteria

S. N.	Nanoparticles	Test organism	Zone of inhibition (mm)				
			Trial-1	Trial-2	Trial-3	Average	Cloxacillin
1	ZnO/Cuo (WE)	*S. aureus*	18	17	15	16.67	23
		P.aeroginosa	16	14	16	15.33	22
2	ZnO/CuO (WoE)	*S. aureus*	15	12	14	13.70	20
		P.aeroginosa	17	13	16	15.30	22
3	ZnO (WE)	*S. aureus*	12	13	13	12.70	22
		P. aeroginosa	15	14	16	15.00	23
4	ZnO (WoE)	*S. aureus*	15	14	15	14.70	22
		P. aeroginosa	15	17	16	16.00	23
5	CuO (WE)	*S. aureus*	12	11	13	12.00	20
		P.aeroginosa	17	13	16	15.30	23
6	CuO (WoE)	*S. aureus*	15	12	14	13.70	22
		P. aeroginosa	11	12	14	12.30	21

Thus, the antibacterial effectiveness is derictly correlated to NPs/NCs particle sizes. The smaller particle size could easily penetrate bacterial cellwall and flourish better effect on bacterial growth (Huang et al., 2022). Generally, the bacterial inhibition mechanism of ZnO/CuO NCs synthesized via the green route, the active oxygen species is the one that could demolish the bacterial cell membranes and inhibit its growth (Bala et al., 2015, Sawai, 2003, Kiwi and Nadtochenko, 2005). Concerning ZnO/CuO (WE) NCs, the antibacterial activity might be ascribed the release of Cu^{2+}-Zn^{2+} ions which interact with negatively charged *S. aureus* bacterial cell (Cai et al., 2014).

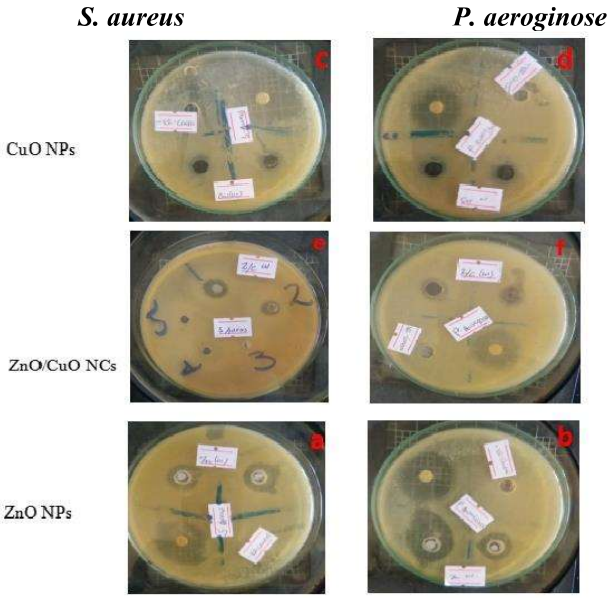

Figure 4. The antibacterial activity of nanoparticles without orange peel extracts against two human pathogenic bacteria

Besides to the above reason, the smaller NPs sizes in fact helped adhering to the bacterial organs so as to devastate the cellwall (Saif et al., 2021). The vital bacterial enzyme would be damaged by NPs that can enter the cell membrane (Sondi and Salopek-Sondi, 2004). Similarly, the *P. aeroginose* strains are highly vulnerable to the phytochemical of orange peel extract which could adhered to the surface of ZnO (WE) and CuO (WE) NPs. The study revealed that the phytochemicals can forms complex structures within the bacterial cellwall and increases cell membrane leaching (Walsh et al., 2003).

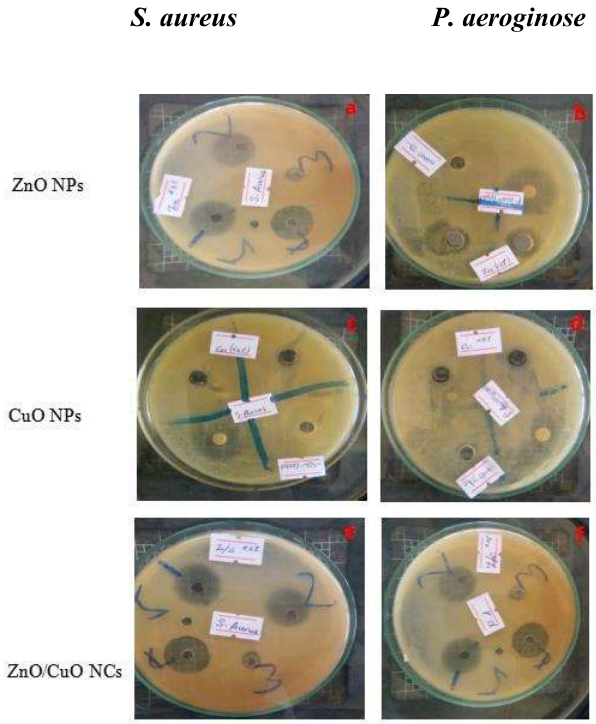

Figure 5. The antibacterial activity of nanoparticles with orange peel extracts against human pathogens

In addition, the hydroxylation of the cellwall could be initiated by OH group of polyphenols which is toxic to bacterial cell wall (Bala et al., 2015). It was evident that the ZOI of samples specified that the synthesized compounds significantly inhibited the targeted bacteria which ascribed to their larger surface area, ROS and particle size (Espitia et al., 2012) which provides better contact with microorganisms. The current finding indicates that the green synthesized ZnO/CuO (WE) NCs could solve serious problems related to human health and promising nanocomposites to curtail such challenges and could substitute antibiotics resistant, economically viable, and toxic to bacterial strains.

Conclusion

In this paper, the Authors attempted to examine the antibacterial activity of green synthesized ZnO NPs, CuO NPs, and ZnO/CuO NCs for the growth inhibition against *Staphylococcus aureus* and *Pseudomonas aeroginosa* bacterial strains while the surface properties of NPs/NCs were characterized with the help of XRD, FTIR and UV-vis spectroscopies. Accordingly, the

XRD has demonstrated the formation of hexagonal wurtzite structure with the crystallite size of 16.46 - 22.71 nm particularly for ZnO/CuO (WE) NCs whereas the FTIR revealed the vibrational stretching indicated the existence of metals-O bonds within the nanomaterials. Similarly, the UV-Vis spectroscopy confirmed the green synthesized ZnO/CuO NCs obssessed a very narrow energy gap. Among those nanomaterials, the one consisted the orange fruit peel has exhibited a remarkable bacterial growth inihibition ability against human pathogens. Concecuently, the highest bacterial growth inhibition zones were recorded by ZnO/CuO (WE) NCs whereas ZnO (WoE, WE), CuO (WoE, WE), and ZnO/CuO (WoE) were ranked in decreasing order. Finally, the authors concluded that the green synthesized NPs/NCs could be applied as disinfectant agent due to their growth inhibition efficiency against the tested microbial organisms in particular bacterial strains.

Acknowledgments

The authors are grateful to Adama Science and Technology University, Addis Ababa Science and Technology University and Chemistry Department of Ambo University, Ethiopia for their support with laboratory, chemicals/reagents and analytical instrumentals.

References

Abid, N., Khan, A. M., Shujait, S., Chaudhary, K., Ikram, M., Imran, M., Maqbool, M. 2022. Synthesis of nanomaterials using various top-down and bottom-up approaches, influencing factors, advantages, and disadvantages: A review. Advances in Colloid and Interface Science, 300, 102597.

Ahamed, M., Alhadlaq, H. A., Khan, M., Karuppiah, P., and Al-Dhabi, N. A. 2014. Synthesis, characterization, and antimicrobial activity of copper oxide nanoparticles. Journal of Nanomaterials.

Ahmed, A. A., Rizvi, Z. R., Shahzad, H., and Farrukh, M. A. 2022. Neodymium oxide nanoparticles synthesis using phytochemicals of leaf extracts of different plants as reducing and capping agents: Growth mechanism, optical, structural and catalytic properties. Journal of the Chinese Chemical Society, 69(3), 462-475.

Akhavan, O., and Ghaderi, E. 2010. Cu and CuO nanoparticles immobilized by silica thin films as antibacterial materials and photocatalysts. Surface and Coatings Technology, 205(1), 219-223.

Albrecht, M. A., Evans, C. W., and Raston, C. L. 2006. Green chemistry and the health implications of nanoparticles. Green chemistry, 8(5), 417-432.

Alkaladi, A., Abdelazim, A. M., and Afifi, M. 2014. Antidiabetic activity of zinc oxide and silver nanoparticles on streptozotocin-induced diabetic rats. International journal of molecular sciences, 15(2), 2015-2023.

Alsafari, I. A., Chaudhary, K., Warsi, M. F., Warsi, A.-Z., Waqas, M., Hasan, M., Shahid, M. 2023. A facile strategy to fabricate ternary WO3/CuO/rGO nano-composite for the enhanced photocatalytic degradation of multiple organic pollutants and antimicrobial activity. Journal of Alloys and Compounds, 938, 168537. doi: ttps://doi.org/10.1016/j.jallcom.2022.168537

Arakha, M., Saleem, M., Mallick, B. C., and Jha, S. 2015. The effects of interfacial potential on antimicrobial propensity of ZnO nanoparticle. Scientific reports, 5(1), 1-10.

Asamoah, J. K. K., Owusu, M. A., Jin, Z., Oduro, F., Abidemi, A., and Gyasi, E. O. 2020. Global stability and cost-effectiveness analysis of COVID-19 considering the impact of the environment: using data from Ghana. Chaos, Solitons and Fractals, 140, 110103.

Awwad, A. M., Salem, N. M., and Abdeen, A. O. 2012. Biosynthesis of silver nanoparticles using Olea europaea leaves extract and its antibacterial activity. Nanoscience and Nanotechnology, 2(6), 164-170.

Azam, A., Ahmed, A. S., Oves, M., Khan, M. S., Habib, S. S., and Memic, A. 2012. Antimicrobial activity of metal oxide nanoparticles against Gram-positive and Gram-negative bacteria: a comparative

study. International journal of nanomedicine, 7, 6003.

Baek, Y.-W., and An, Y.-J. 2011. Microbial toxicity of metal oxide nanoparticles (CuO, NiO, ZnO, and Sb2O3) to Escherichia coli, Bacillus subtilis, and Streptococcus aureus. Science of the total environment, 409(8), 1603-1608.

Baker-Austin, C., Wright, M. S., Stepanauskas, R., and McArthur, J. 2006. Co-selection of antibiotic and metal resistance. Trends in microbiology, 14(4), 176-182.

Bala, N., Saha, S., Chakraborty, M., Maiti, M., Das, S., Basu, R., and Nandy, P. 2015. Green synthesis of zinc oxide nanoparticles using Hibiscus subdariffa leaf extract: effect of temperature on synthesis, anti-bacterial activity and anti-diabetic activity. RSC Advances, 5(7), 4993-5003.

Balouiri, M., Sadiki, M., Ibnsouda, S.K. (2016); Methods for in vitro evaluating antimicrobial activity : A review $. *Journal of Pharmaceutical Analysis* *6*(2); 71-79. **https://doi.org/10.1016/j.jpha.2015.11.005**

Batool, S., Hasan, M., Dilshad, M., Zafar, A., Tariq, T., Wu, Z., Shu, X. 2022. Green synthesis of Cordia myxa incubated ZnO, Fe_2O_3, and Co_3O_4 nanoparticle: Characterization, and their response as biological and photocatalytic agent. Advanced Powder Technology, 33(11), 103780. doi: **https://doi.org/10.1016/j.apt.2022.103780**

Cai, Y., Strømme, M., Melhus, Å., Engqvist, H., and Welch, K. 2014. Photocatalytic inactivation of biofilms on bioactive dental adhesives. Journal of Biomedical Materials Research Part B: Applied Biomaterials, 102(1), 62-67.

Cui, Y., Li, H., Li, Y., and Mao, L. 2022. Novel insights into nanomaterials for immunomodulatory bone regeneration. Nanoscale Advances, 4(2), 334-352.

Dadi, R., Azouani, R., Traore, M., Mielcarek, C., and Kanaev, A. 2019. Antibacterial activity of ZnO and CuO nanoparticles against gram positive and gram negative strains. Materials Science and Engineering: C, 104, 109968.

Das, R. K., Gogoi, N., Babu, P. J., Sharma, P., Mahanta, C., and Bora, U. 2012. The synthesis of gold nanoparticles using Amaranthus spinosus leaf extract and study of their optical properties.

Devi, P. B., Vijayabharathi, R., Sathyabama, S., Malleshi, N. G., and Priyadarisini, V. B. 2014. Health benefits of finger millet (Eleusine coracana L.) polyphenols and dietary fiber: a review. Journal of food science and technology, 51(6), 1021-1040.

Dey, A. 2018. Semiconductor metal oxide gas sensors: A review. Materials Science and Engineering: B, 229, 206-217.

Díaz-Visurraga, J., Gutiérrez, C., Von Plessing, C., and García, A. 2011. Metal nanostructures as antibacterial agents. Science against microbial pathogens: communicating current research and technological advances, 1, 210-218.

Espitia, P. J. P., Soares, N. d. F. F., Coimbra, J. S. d. R., de Andrade, N. J., Cruz, R. S., and Medeiros, E. A. A. 2012. Zinc oxide nanoparticles: synthesis, antimicrobial activity and food packaging applications. Food and bioprocess technology, 5(5), 1447-1464.

Fahmy, B., and Cormier, S. A. (2009). Copper oxide nanoparticles induce oxidative stress and cytotoxicity in airway epithelial cells. Toxicology in vitro, 23(7), 1365-1371.

Faisal, S., Jan, H., Shah, S. A., Shah, S., Khan, A., Akbar, M. T., Akhtar, N. 2021. Green synthesis of zinc oxide (ZnO) nanoparticles using aqueous fruit extracts of Myristica fragrans: their characterizations and biological and environmental applications. ACS omega, 6(14), 9709-9722.

Gawade, V., Gavade, N., Shinde, H., Babar, S., Kadam, A., and Garadkar, K. 2017. Green synthesis of ZnO nanoparticles by using Calotropis procera leaves for the photodegradation of methyl orange. Journal of Materials Science: Materials in Electronics, 28(18), 14033-14039.

Gayen, R., Das, S., Dalui, S., Bhar, R., and Pal, A. 2008. Zinc magnesium oxide nanofibers on glass substrate by solution growth technique. Journal of crystal growth, 310(18), 4073-4080.

Gold, K., Slay, B., Knackstedt, M., and Gaharwar, A. K. 2018. Antimicrobial activity of metal and metal-oxide based nanoparticles. Advanced Therapeutics, 1(3), 1700033.

Hajiali, H., Ouyang, L., Llopis-Hernandez, V., Dobre, O., and Rose, F. R. 2021. Review of emerging nanotechnology in bone regeneration: progress, challenges, and perspectives. Nanoscale, 13(23), 10266-10280.

Hajipour, M. J., Fromm, K. M., Ashkarran, A. A., de Aberasturi, D. J., de Larramendi, I. R., Rojo, T., Mahmoudi, M. 2012. Antibacterial properties of nanoparticles. TRENDS in Biotechnology, 30(10), 499-511.

Hasan, M., Zafar, A., Imran, M., Iqbal, K. J., Tariq, T., Iqbal, J., Shu, X. 2022. Crest to Trough Cellular Drifting of Green-Synthesized Zinc Oxide and Silver Nanoparticles. ACS omega, 7(39), 34770-34778. doi: 10.1021/acsomega.2c02178

Hashmi, H. F. 2021. Qualitative and Quantitative Analysis of Phytochemicals in Lepidium Pinnatifidum Ledeb. Sch Int J Tradit Complement Med, 4(5), 67-75.

Herlekar, M., Barve, S., and Kumar, R. 2014. Plant-mediated green synthesis of iron nanoparticles. Journal of Nanoparticles, 2014.

Huang, L., Chen, R., Luo, J., Hasan, M., and Shu, X. 2022. Synthesis of phytonic silver nanoparticles as bacterial and ATP energy silencer. Journal of Inorganic Biochemistry, 231, 111802. doi: **https://doi.org/10.1016/j.jinorgbio.2022.111802**

Huh, A. J., and Kwon, Y. J. 2011. "Nanoantibiotics": a new paradigm for treating infectious diseases using nanomaterials in the antibiotics resistant era. Journal of controlled release, 156(2), 128-145.

Hussain, I., Singh, N., Singh, A., Singh, H., and Singh, S. 2016. Green synthesis of nanoparticles and its potential application. Biotechnology letters, 38(4), 545-560.

Hussain, R., Hasan, M., Iqbal, K. J., Zafar, A., Tariq, T., Saif, M. S., Anjum, S. I. 2023. Nano-managing silver and zinc as bio-conservational approach against pathogens of the honey bee. J Biotechnol, 365, 1-10. doi: 10.1016/j.jbiotec.2023.01.009

Hussain, R., Zafar, A., and Hasan, M. 2023. Casting Zinc Oxide Nanoparticles Using Fagonia Blend Microbial Arrest. 195(1), 264-282. doi: 10.1007/s12010-022-04152-8

Jiang, W., Mashayekhi, H., and Xing, B. 2009. Bacterial toxicity comparison between nano-and micro-scaled oxide particles. Environmental pollution, 157(5), 1619-1625.

Joshi, R. S., Gupta, V. S., and Giri, A. P. 2014. Differential antibiosis against Helicoverpa armigera exerted by distinct inhibitory repeat domains of Capsicum annuum proteinase inhibitors. Phytochemistry, 101, 16-22.

Kasemets, K., Ivask, A., Dubourguier, H.-C., and Kahru, A. 2009. Toxicity of nanoparticles of ZnO, CuO and TiO2 to yeast Saccharomyces cerevisiae. Toxicology in vitro, 23(6), 1116-1122.

Khan, H. A. A., Shad, S. A., and Akram, W. 2013. Resistance to new chemical insecticides in the house fly, Musca domestica L., from dairies in Punjab, Pakistan. Parasitology research, 112(5), 2049-2054.

Khan, M., Ngo, H. H., Guo, W., Liu, Y., Nghiem, L. D., Hai, F. I., Wu, Y. 2016. Optimization of process parameters for production of volatile fatty acid, biohydrogen and methane from anaerobic digestion. Bioresource technology, 219, 738-748.

Kiwi, J., and Nadtochenko, V. 2005. Evidence for the mechanism of photocatalytic degradation of the bacterial wall membrane at the TiO_2 interface by ATR-FTIR and laser kinetic spectroscopy. Langmuir, 21(10), 4631-4641.

Kumar, C. R., Betageri, V. S., Nagaraju, G., Pujar, G., Onkarappa, H., and Latha, M. 2020. One-pot green synthesis of ZnO–CuO nanocomposite and their enhanced photocatalytic and antibacterial activity. Advances in Natural Sciences: Nanoscience and Nanotechnology, 11(1), 015009.

Kumar Mandal, R., Ghosh, S., and Pal Majumder, T. 2023. Comparative study

between degradation of dyes (MB, MO) in monotonous and binary solution employing synthesized bimetallic (Fe-CdO) NPs having antioxidant property. Results in Chemistry, 5, 100788. doi: **https://doi.org/10.1016/j.rechem.2023.100788**

Kumar, S., Beena, A., Awana, M., and Singh, A. 2017. Physiological, biochemical, epigenetic and molecular analyses of wheat (Triticum aestivum) genotypes with contrasting salt tolerance. Frontiers in Plant Science, 8, 1151.

Lewis, K., and Klibanov, A. M. 2005. Surpassing nature: rational design of sterile-surface materials. TRENDS in Biotechnology, 23(7), 343-348.

Li, J., Tan, L., Liu, X., Cui, Z., Yang, X., Yeung, K. W. K., Wu, S. 2017. Balancing bacteria–osteoblast competition through selective physical puncture and biofunctionalization of ZnO/polydopamine/arginine-glycine-aspartic acid-cysteine nanorods. Acs Nano, 11(11), 11250-11263.

Li, M., Zhu, L., and Lin, D. 2011. Toxicity of ZnO nanoparticles to Escherichia coli: mechanism and the influence of medium components. Environmental science and technology, 45(5), 1977-1983.

Liang, F.-X., Gao, Y., Xie, C., Tong, X.-W., Li, Z.-J., and Luo, L.-B. 2018. Recent advances in the fabrication of graphene–ZnO heterojunctions for optoelectronic device applications. Journal of Materials Chemistry C, 6(15), 3815-3833.

Lipovsky, A., Nitzan, Y., Gedanken, A., and Lubart, R. 2011. Antifungal activity of ZnO nanoparticles—the role of ROS mediated cell injury. Nanotechnology, 22(10), 105101.

Lu, C., Brauer, M. J., and Botstein, D. 2009. Slow growth induces heat-shock resistance in normal and respiratory-deficient yeast. Molecular biology of the cell, 20(3), 891-903.

Mahmood, F., Zehra, S. S., Hasan, M., Zafar, A., Tariq, T., Abdullah, M., Shu, X. 2023. Bioinspired Cobalt Oxide Nanoball Synthesis, Characterization, and Their Potential as Metal Stress Absorbants. ACS omega, 8(6), 5836-5849. doi: 10.1021/acsomega.2c07545

Mukherjee, S., Sushma, V., Patra, S., Barui, A. K., Bhadra, M. P., Sreedhar, B., and Patra, C. R. 2012. Green chemistry approach for the synthesis and stabilization of biocompatible gold nanoparticles and their potential applications in cancer therapy. Nanotechnology, 23(45), 455103.

Multari, S., Licciardello, C., Caruso, M., and Martens, S. 2020. Monitoring the changes in phenolic compounds and carotenoids occurring during fruit development in the tissues of four citrus fruits. Food Research International, 134, 109228.

Naik, M. M., Naik, H., Nagaraju, G., Vinuth, M., Vinu, K., and Rashmi, S. 2018. Effect of aluminium doping on structural, optical, photocatalytic and antibacterial activity on nickel ferrite nanoparticles by sol–gel auto-combustion method. Journal of Materials Science: Materials in Electronics, 29(23), 20395-20414.

Nair, S., Sasidharan, A., Divya Rani, V., Menon, D., Nair, S., Manzoor, K., and Raina, S. 2009. Role of size scale of ZnO nanoparticles and microparticles on toxicity toward bacteria and osteoblast cancer cells. Journal of Materials Science: Materials in Medicine, 20(1), 235-241.

Prabakaran, S., Lippens, G., Steen, H., and Gunawardena, J. 2012. Post-translational modification: nature's escape from genetic imprisonment and the basis for dynamic information encoding. Wiley Interdisciplinary Reviews: Systems Biology and Medicine, 4(6), 565-583.

Rajiv, P., Rajeshwari, S., and Venckatesh, R. 2013. Bio-Fabrication of zinc oxide nanoparticles using leaf extract of Parthenium hysterophorus L. and its size-dependent antifungal activity against plant fungal pathogens. Spectrochimica Acta Part A: Molecular and Biomolecular Spectroscopy, 112, 384-387.

Saif, M. S., Zafar, A., Waqas, M., Hassan, S. G., Haq, A. u., Tariq, T., Shu, X. 2021. Phyto-reflexive Zinc Oxide Nano-Flowers synthesis: An advanced photocatalytic degradation and infectious therapy. Journal of Materials Research and Technology, 13, 2375-2391. doi:

https://doi.org/10.1016/j.jmrt.2021.05.107

Sankapal, B. R., Gajare, H. B., Karade, S. S., Salunkhe, R. R., and Dubal, D. P. 2016. Zinc oxide encapsulated carbon nanotube thin films for energy storage applications. Electrochimica Acta, 192, 377-384.

Sawai, J. 2003. Quantitative evaluation of antibacterial activities of metallic oxide powders (ZnO, MgO and CaO) by conductimetric assay. Journal of microbiological methods, 54(2), 177-182.

Shafique, S., Jabeen, N., Ahmad, K. S., Irum, S., Anwaar, S., Ahmad, N., Hussain, S. Z. (2020). Green fabricated zinc oxide nanoformulated media enhanced callus induction and regeneration dynamics of Panicum virgatum L. Plos one, 15(7), e0230464.

Shah, N. I., Jabeen, N., Irum, S., Ahmad, K. S., Tauseef, I., Khan, T. F., Mehmood, A. 2021. Environmentally benign and economical bio-fabrication of ZnO and Cr-doped ZnO nanoparticles using leaf extract of Citrus reticulata for biological activities. Materials Today Communications, 27, 102383.

Shamsuzzaman, A., Amin, R. S., Calvin, A. D., Davison, D., and Somers, V. K. 2014. Severity of obstructive sleep apnea is associated with elevated plasma fibrinogen in otherwise healthy patients. Sleep and Breathing, 18(4), 761-766.

Sondi, I., and Salopek-Sondi, B. 2004. Silver nanoparticles as antimicrobial agent: a case study on E. coli as a model for Gram-negative bacteria. Journal of colloid and interface science, 275(1), 177-182.

Thi, T. U. D., Nguyen, T. T., Thi, Y. D., Thi, K. H. T., Phan, B. T., and Pham, K. N. 2020. Green synthesis of ZnO nanoparticles using orange fruit peel extract for antibacterial activities. RSC Advances, 10(40), 23899-23907.

Veisi, H., Karmakar, B., Tamoradi, T., Hemmati, S., Hekmati, M., and Hamelian, M. 2021. Biosynthesis of CuO nanoparticles using aqueous extract of herbal tea (Stachys Lavandulifolia) flowers and evaluation of its catalytic activity. Scientific reports, 11(1), 1-13.

Von Nussbaum, F., Brands, M., Hinzen, B., Weigand, S., and Häbich, D. 2006. Antibacterial natural products in medicinal chemistry—exodus or revival? Angewandte Chemie International Edition, 45(31), 5072-5129.

Walsh, S. E., Maillard, J. Y., Russell, A., Catrenich, C., Charbonneau, D., and Bartolo, R. 2003. Activity and mechanisms of action of selected biocidal agents on Gram-positive and-negative bacteria. Journal of applied microbiology, 94(2), 240-247.

Whitesides, G. M. 2005. Nanoscience, nanotechnology, and chemistry. Small, 1(2), 172-179.

Xiang, Y., Li, J., Liu, X., Cui, Z., Yang, X., Yeung, K., Wu, S. 2017. Construction of poly (lactic-co-glycolic acid)/ZnO nanorods/Ag nanoparticles hybrid coating on Ti implants for enhanced antibacterial activity and biocompatibility. Materials Science and Engineering: C, 79, 629-637.

Yoon, S. H., and Kim, D.-J. 2006. Fabrication and characterization of ZnO films for biological sensor application of FPW device. Paper presented at the 2006 15th ieee international symposium on the applications of ferroelectrics.